Study on Extraction Behavior of Lithium Chloride by Tri-*n*-butyl Phosphate Dissolved in Kerosene

Ting-Chia Huang* and Teh-Hua Tsai

Department of Chemical Engineering, National Cheng Kung University, Tainan, Taiwan 70101, Republic of China

The extraction behavior of lithium chloride from aqueous solutions by tri-*n*-butyl phoshate (TBP) dissolved in kerosene has been studied systematically at 25 °C. The distribution ratios of lithium chloride increase with both the concentrations of lithium chloride in the aqueous solutions and tri-*n*-butyl phosphate in the organic solutions increasing. In addition to the water content determination, physical property measurements of densities, viscosities, and conductivities of the aqueous phase and organic phase are carried out. From quantitative analysis, three extracted species are found to exist in the organic solutions. At first, the composition $LiCl\cdot(TBP)_3\cdot(H_2O)_4$ is formed at lower initial aqueous lithium chloride concentrations. And then, $(LiCl)_2\cdot(TBP)_3\cdot(H_2O)_4$ is formed at higher lithium chloride concentrations. Finally, the aggregation of $(LiCl)_2\cdot(TBP)_3\cdot(H_2O)_4$ is formed near the saturated lithium chloride solutions.

Introduction

Tri-*n*-butyl phosphate (abbreviated as TBP) has been studied extensively as a neutral or solvation extractant in hydrometallurgical processes for the separation and purification of a number of metals, especially in familiar nuclear fuel reprocessing (*1-3*).

The extraction of lithium chloride with TBP has been studied by Baldwin et al. (*4*) and Morris and Short (*5*). Baldwin et al. (*4*) studied the extraction of lithium chloride by TBP dissolved in *n*-hexane and found that the extraction behavior was dependent upon whether or not water accompanies the electrolyte into the TBP. Morris and Short (*5*) studied the extraction of lithium chloride by TBP dissolved in benzene at 20 °C; they reported that, at higher concentrations, TBP molecules begin to substitute for H_2O molecules in the solvation shell of the extracted lithium chloride, but a total solvation number of 4 seems to be maintained.

McKay et al. (*6*) proposed that the interaction of water and TBP was through the complex $TBP\cdot H_2O$ for dilute TBP systems and $(TBP)_2\cdot H_2O$ for small amounts of water in high concentrations of TBP. On the other hand, they found a $(TBP)_2\cdot(H_2O)_2$ complex at higher water concentrations. Roddy (*7*) studied the extraction of water into TBP and octane. He suggested that at least five species were formed in the TBP-water system by computer analyses: TBP, $TBP\cdot H_2O$, $(TBP)_2\cdot(H_2O)_2$, $(TBP)_4\cdot(H_2O)_4$, and $(TBP)_2\cdot H_2O$.

In the present study we examine the extraction behavior of lithium chloride from aqueous solutions by tri-*n*-butyl phosphate dissolved in kerosene. We try to establish the compositions and chemical reactions of the lithium chloride extracted from the aqueous phase by tri-*n*-butyl phosphate. The influence of the equilibrium concentration of lithium chloride in the aqueous phase and TBP in the organic phase on the distribution ratios is investigated. We also study the hydration of the compounds extracted in the organic phase by chemical methods with the Karl-Fischer reagent (*8*). Alternately, densities, viscosities, and conductivities of both the aqueous and organic phases are determined in order to reconfirm the composition of the species extracted.

Experimental Section

Materials. Tri-*n*-butyl phosphate used in this work was the product of Hayashi Pure Chemical Industries, Ltd., Osaka, Japan. It was purified by washing with 5% sodium carbonate solution and then with distilled water. Kerosene (density = 785.4 kg/m^3, boiling range = 200-250 °C; the product of Chinese Petroleum Co., Taiwan, ROC) was washed twice with 1/5 volume 98% H_2SO_4 and then with distilled water until it was neutral (*9*). The other inorganic chemicals were analytical reagent grade supplied by Hayashi.

Measurements of the Distribution Ratio of Lithium Chloride. A 20-mL amount (2.0×10^{-5} m^3) of the organic solution and an equal volume of aqueous solution were mixed in glass flasks with ground-glass stoppers and shaken by a mechanical shaker for at least 30 min at 25.0 ± 0.1 °C. Preliminary experiments showed the time needed to reach equilibrium to be less than 15 min. The two phases were separated after they had been allowed to settle for 4 h in a thermostat at 25.0 ± 0.1 °C.

Since the initial aqueous solutions contained only lithium chloride, i.e., $[Li^+] = [Cl^-]$, therefore, one can determine either the lithium or chloride concentration as total concentration of lithium chloride. After phase separation, the concentration of lithium was measured with the IL-551 atomic absorption spectrophotometer (Instrumentation Laboratory Inc.) at the wavelength of 670.8 nm for lower concentrations. At higher concentrations, each solution was analyzed for chloride content by the Fajans method or adsorption indicator method (*10*, *11*). All analyses were performed in duplicate.

Measurements of Density, Viscosity, and Conductivity. The densities of both phases were determined by means of an Ostwald specific gravity bottle at 25.0 ± 0.1 °C. The density values obtained were used to calculate the values of viscosity.

An Ostwald capillary viscometer calibrated with pure water was used to determine the viscosities of both the aqueous and organic phases in a thermostatic water bath at 25.0 ± 0.1 °C. The time of flow between calibration marks was measured to within 0.01 s with a stopwatch.

The conductivities of both phases were measured with a Corning 220 conductivity meter (Corning Limited Halstead Essex Co.) calibrated with 0.1 kmol/m^3 KCl at 25.0 ± 0.1 °C.

Measurements of the Water Content in the Organic Phase. The water in the organic phase was titrated by means of a Karl-Fischer reagent (*8*), using the dead-stop end point method as determined with a Karl-Fischer titrimeter (Swiss Metrohm Co., Ltd.). The reagent was standardized against a known solution of water in methanol. Duplicate trials showed that the results were reproducible to within 2% or better.

Results and Discussion

Distribution Ratio of Lithium Chloride. In the absence of kerosene, the extraction equilibrium of lithium chloride by tri-*n*-butyl phosphate is studied at 25 °C. The molar concentrations of lithium chloride in the initial aqueous solutions and in both the equilibrium organic and aqueous phases are listed in Table I.

* To whom correspondence should be addressed.

0021-9568/91/1736-0231$02.50/0

Table I. Dependence of Distribution Ratios of LiCl D_{LiCl} on the Initial ($[LiCl]_i$) and Equilibrium ($[LiCl]_{aq}$ and $[LiCl]_{org}$) Concentrations (kmol/m³) of Lithium Chloride in the Aqueous Phase and TBP Phase at Constant Initial TBP Concentration ($[\overline{TBP}]_i$ = 3.41 kmol/m³) and 25 °C

expt no.	$[LiCl]_i$	$[LiCl]_{aq}$	$[LiCl]_{org}$	D_{LiCl}
1	0	0	0	0
2	0.6932	0.6990	0.000 405	0.000 580
3	1.383	1.384	0.001 216	0.000 878
4	2.069	2.077	0.002 836	0.001 366
5	2.752	2.765	0.005 470	0.001 978
6	3.432	3.454	0.010 33	0.002 991
7	4.108	4.093	0.018 44	0.004 505
8	4.781	4.741	0.031 81	0.006 709
9	5.451	5.409	0.053 08	0.009 813
10	6.117	6.058	0.096 24	0.015 89
11	6.780	6.625	0.156 0	0.023 55
12	7.477	7.334	0.276 5	0.037 71
13	8.176	7.830	0.443 7	0.056 66
14	8.880	8.509	0.664 5	0.078 10
15	9.586	9.056	0.821 5	0.090 72
16	10.30	9.613	1.044	0.108 6
17	11.01	10.043	1.210	0.120 5
18	11.73	10.66	1.425	0.133 7
19	12.45	11.39	1.556	0.136 6
20	13.17	12.04	1.764	0.146 5
21	13.90	12.92	1.939	0.150 0
22	14.24	13.15	2.041	0.155 2
23	saturated	14.32	2.206	0.154 0

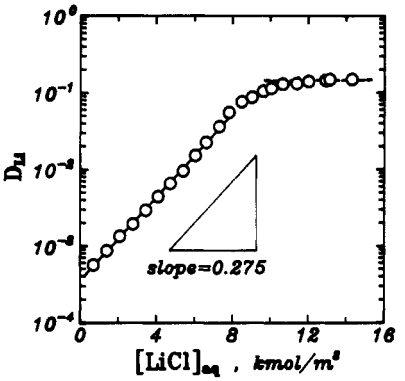

Figure 1. Dependence of distribution ratios of lithium chloride in the equilibrium aqueous phase at $[\overline{TBP}]_i$ = 3.41 kmol/m³ and 25 °C.

The distribution ratios of lithium chloride are calculated according to the following equation and shown in the last column of Table I.

$$D_{LiCl} = \frac{\text{total amt of LiCl in organic phase}}{\text{total amt of LiCl in aqueous phase}} = \frac{[LiCl]_{org}}{[LiCl]_{aq}} = \frac{[\overline{LiCl}]}{[LiCl]} \quad (1)$$

Figure 1 shows the distribution ratios versus the equilibrium concentration of lithium chloride in the aqueous solutions. The results show that the distribution ratios increase at first with the increase of lithium chloride concentration in the equilibrium aqueous solution and then reach a constant value. When $[LiCl]_{aq} < 8$ kmol/m³, the distribution ratios of lithium chloride between the TBP phase and the aqueous phase at 25 °C can be expressed as

$$D_{LiCl} = 3.510 \times 10^{-4} \exp((0.6340\ m^3/kmol)[LiCl]_{aq}) \quad (2)$$

Density, Viscosity, and Conductivity of Equilibrium Phases. The densities, viscosities, and conductivities of the equilibrium organic phase and aqueous phase for LiCl between water and

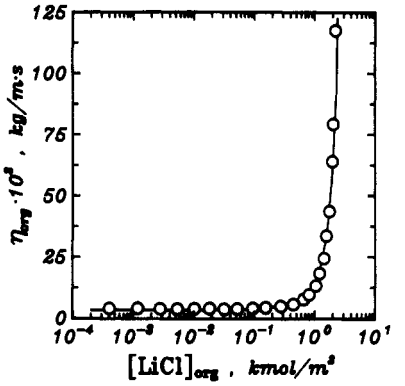

Figure 2. Variation in the viscosity of the equilibrium organic phase as a function of the concentration of lithium chloride extracted in the organic phase at $[\overline{TBP}]_i$ = 3.41 kmol/m³ and 25 °C.

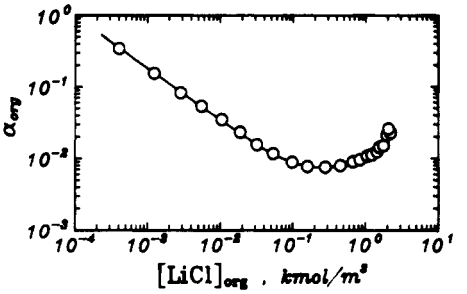

Figure 3. Dependence of the degree of association of lithium chloride in the equilibrium organic phase at $[\overline{TBP}]_i$ = 3.41 kmol/m³ and 25 °C.

TBP are measured for various LiCl concentrations at 25 °C and at constant initial TBP concentration ($[\overline{TBP}]_i$ = 3.41 kmol/m³). The results are tabulated in Table II. The densities of both the equilibrium phases are proportional to the concentrations of lithium chloride, as can be seen from columns 2 and 3 in Table II. By means of curve fitting, the relationships between densities and concentrations of lithium chloride can be expressed as

$$\rho_{aq} = (21.06\ kg/kmol)[LiCl]_{aq} + 1003\ (kg/m^3) \quad (3)$$

$$\rho_{org} = (27.10\ kg/kmol)[LiCl]_{org} + 977.1\ (kg/m^3) \quad (4)$$

The plot of viscosity against equilibrium concentration of lithium chloride in the organic phase is shown in Figure 2. It shows a break point at approximately 1.7 kmol/m³ of lithium chloride in the organic phase. These phenomena can be described as the LiCl complex of TBP tends to form large polymeric species in a fully loaded organic phase at high concentration of lithium chloride.

The equivalent conductances (Λ) are obtained from the relationship of $\Lambda = \kappa V$, where κ is specific conductance, and V is equivalent molar volume. The calculated equivalent conductances of the equilibrium aqueous phase and organic phase for LiCl between water and TBP at constant initial TBP concentration ($[\overline{TBP}]_i$ = 3.41 kmol/m³) and 25 °C are tabulated in columns 8 and 9 of Table II. By means of curve fitting, the relationships between the equivalent conductances and concentrations of lithium chloride for the equilibrium phases can be expressed as

$$\Lambda_{aq} = 7.271 \exp((-0.1742\ m^3/kmol)[LiCl]_{aq}) \quad (5)$$

$$\Lambda_{org} = 3.603 \times 10^{-3}([LiCl]_{org})^{-0.6268} \quad (6)$$

The degree of dissociation, α, can be obtained by Walden's equation (*12*), $\alpha = 1000\Lambda\eta/6$, which is tabulated in the last

Table II. Densities, Viscosities, Conductivities, and Degrees of Dissociation (α_{org}) of the Equilibrium Aqueous Phase and Organic Phase at Constant Initial TBP Concentration ($[\overline{TBP}]_i$ = 3.41 kmol/m³) and 25 °C

	density, 10^3 kg/m³		viscosity, 10^{-3} kg/(m·s)		specific conductance, 1/(Ω·m)		equivalent conductance, m²/(Ω·kmol)		
expt no.	ρ_{aq}	ρ_{org}	η_{aq}	η_{org}	κ_{aq}	$10^3\kappa_{org}$	Λ_{aq}	Λ_{org}	α_{org}
1	0.9971	0.9722	0.8937	3.760	0.000159	0.029			
2	1.015	0.9740	0.9569	3.713	4.38	0.225	6.27	0.555	0.344
3	1.032	0.9757	1.037	3.717	7.92	0.301	5.72	0.248	0.153
4	1.051	0.9772	1.142	3.589	10.22	0.389	4.92	0.137	0.0820
5	1.068	0.9761	1.263	3.560	11.96	0.495	4.33	0.0905	0.0537
6	1.078	0.9768	1.369	3.596	13.25	0.594	3.84	0.0575	0.0345
7	1.090	0.9776	1.482	3.602	14.78	0.712	3.61	0.0386	0.0232
8	1.101	0.9791	1.617	3.608	15.20	0.828	3.21	0.0260	0.0157
9	1.115	0.9800	1.783	3.645	15.45	1.017	2.86	0.0192	0.0116
10	1.130	0.9813	1.955	3.818	15.37	1.349	2.54	0.0140	0.00892
11	1.142	0.9829	2.097	4.068	15.35	1.777	2.32	0.0114	0.00772
12	1.157	0.9861	2.323	4.757	15.04	2.66	2.05	0.00962	0.00763
13	1.168	0.9889	2.545	5.724	14.67	3.67	1.87	0.00827	0.00789
14	1.182	0.9944	2.630	7.551	14.63	4.72	1.72	0.00710	0.00894
15	1.194	0.9996	2.935	9.473	13.07	4.96	1.44	0.00604	0.00953
16	1.206	1.0049	3.281	13.14	12.48	5.10	1.30	0.00488	0.0107
17	1.216	1.010	3.608	18.24	13.13	4.44	1.31	0.00367	0.0112
18	1.229	1.015	3.970	24.41	13.16	4.37	1.23	0.00307	0.0125
19	1.242	1.020	4.541	33.60	13.29	4.02	1.17	0.00258	0.0145
20	1.258	1.025	5.720	43.57	12.51	3.72	1.04	0.00211	0.0153
21	1.274	1.029	8.765	64.11	10.02	3.83	0.775	0.00198	0.0211
22	1.280	1.034	10.17	79.36	9.36	3.98	0.712	0.00195	0.0258
23	1.309	1.036	13.38	118.0	6.44	2.56	0.450	0.00116	0.0228

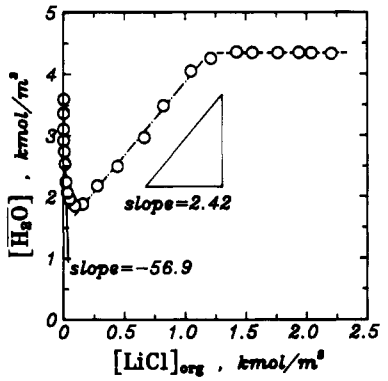

Figure 4. Water extracted into the organic phase against the concentration of lithium chloride extracted in the organic phase at $[\overline{TBP}]_i$ = 3.41 kmol/m³ and 25 °C.

column of Table II. Figure 3 shows the plot of the degree of dissociation against the equilibrium concentration of lithium chloride in the organic phase. It indicates that the lithium chloride exists to a large extent in molecular form or as ion pairs in the organic phase, and the degree of dissociation varies between 0.00763–0.344%.

Water Content of the TBP Phase. The concentration of water in the organic phase, $[\overline{H_2O}]$, is measured by using the Karl-Fischer reagent, and the results are listed in column 4 of Table III. The relation of water content in the organic phase versus equilibrium concentration of lithium chloride in the organic phase is shown in Figure 4.

When pure TBP is equilibrated with water, the mole ratio of TBP:H_2O is 1:1. It is shown in row 1 of Table III. It agrees with the results of McKay et al. (*6*), Alcock et al. (*13*), Tuck (*14*), and Kertes (*15*). Figure 4 gives a curve composed of three parts corresponding to low, middle, and high LiCl concentration regions. In the first part of the curve in Figure 4, the negative slope can be attributed to the lowering by lithium chloride of the water activity in the aqueous phase, leading to a resultant decrease in the distribution of water (*16*). The first break point of the curve occurs at 0.09624 kmol/m³ of $[\overline{LiCl}]$, that appears to be offset by increasing extraction of hydrated

Table III. Molar Ratios of LiCl, TBP, and H_2O in the Organic Phase at Constant Initial TBP Concentration ($[\overline{TBP}]_i$ = 3.41 kmol/m³) and 25 °C

expt	concentration, kmol/m³				$[\overline{LiCl}]$: $[\overline{TBP}]$:
no.	$[\overline{LiCl}]$	$[\overline{TBP}]$	$[\overline{H_2O}]$	$[\overline{H_2O}]/[\overline{TBP}]$	$[\overline{H_2O}]$
1	0	3.407	3.596	1.055	
2	0.000405	3.429	3.372	0.9835	1:8460:8320
3	0.001216	3.463	3.114	0.9018	1:2840:2560
4	0.002836	3.471	2.926	0.8430	1:1220:1030
5	0.005470	3.478	2.746	0.7893	1:636:502
6	0.01033	3.494	2.545	0.7284	1:338:246
7	0.01844	3.516	2.250	0.6401	1:191:122
8	0.03181	3.531	2.079	0.5889	1:111:65.4
9	0.05308	3.538	1.972	0.5575	1:66.7:37.2
10	0.09624	3.544	1.857	0.5240	1:36.8:19.3
11	0.1560	3.538	1.886	0.5330	1:22.7:12.1
12	0.2765	3.511	2.188	0.6232	1:12.7:7.91
13	0.4437	3.473	2.500	0.7197	1:7.83:5.62
14	0.6645	3.427	2.974	0.8679	1:5.16:4.48
15	0.8215	3.386	3.499	1.033	1:4.12:4.26
16	1.044	3.333	4.051	1.216	1:3.19:3.88
17	1.210	3.311	4.271	1.290	1:2.74:3.53
18	1.425	3.288	4.370	1.329	1:2.31:3.07
19	1.556	3.287	4.357	1.326	1:2.11:2.80
20	1.764	3.273	4.363	1.333	1:1.86:2.47
21	1.939	3.261	4.365	1.339	1:1.68:2.25
22	2.041	3.262	4.362	1.337	1:1.60:2.14
23	2.206	3.245	4.341	1.338	1:1.47:1.97

LiCl into the organic phase. The ratio of $[\overline{TBP}]$:$[\overline{H_2O}]$ is approximately 2 at this break point. It represents the compound $(\overline{TBP})_2{\cdot}H_2O$ that is formed in the organic phase, which agrees with the results of Tuck (*14*) and Kertes (*15*).

The slope of the second part of the curve in Figure 4 is 2.42, indicating that each lithium chloride molecule is approximately accompanied by $^5/_2$ water molecules on passing from the aqueous phase into TBP. After 1.425 kmol/m³ of LiCl enters the organic phase, the almost horizontal line of the third part of the curve indicates that any further lithium chloride is extracted without accompanying water.

Table IV shows various equilibrium concentrations, distribution ratios, and water contents at constant aqueous phase ($[LiCl]_i$ = 13.9 kmol/m³) and dilute concentrations of TBP in

Table IV. Distribution Ratios and Water Contents at $[LiCl]_i$ = 13.9 kmol/m³ and 25 °C

expt no.	$[\overline{TBP}]_i$, kmol/m³	LiCl molarity, kmol/m³ $[LiCl]_{aq}$	LiCl molarity, kmol/m³ $[LiCl]_{org}$	D_{LiCl}	$[\overline{H_2O}]$, kmol/m³
1	kerosene	13.90	0	0	0
2	0.3420	13.78	0.04356	0.003162	0.06801
3	0.6840	13.73	0.2056	0.01498	0.3086
4	1.026	13.62	0.3849	0.02825	0.6670
5	1.368	13.52	0.5683	0.04202	1.072
6	1.710	13.42	0.7567	0.05638	1.509
7	2.052	13.27	0.9927	0.07481	1.975
8	2.394	13.17	1.212	0.09200	2.466
9	2.736	13.07	1.446	0.1106	3.089
10	3.078	12.92	1.661	0.1286	3.685
11	3.420	12.81	1.872	0.1461	4.360

Table V. Densities, Viscosities, and Conductivities of Equilibrium Aqueous Phase and Organic Phase at 13.9 kmol/m³ of Initial LiCl Concentration and 25 °C

expt no.	density, 10^3 kg/m³ ρ_{aq}	density, 10^3 kg/m³ ρ_{org}	viscosity, 10^{-3} kg/(m·s) η_{aq}	viscosity, 10^{-3} kg/(m·s) η_{org}	specific conductance, 1/(Ω·m) κ_{aq}	specific conductance, 1/(Ω·m) $10^3\kappa_{org}$
1	1.301	0.7854	13.50	1.340	7.87	0.015
2	1.294	0.8049	12.86	1.425	8.26	0.015
3	1.288	0.8321	11.83	1.748	8.52	0.016
4	1.286	0.8554	11.08	2.151	8.94	0.018
5	1.281	0.8805	10.79	2.809	8.73	0.047
6	1.278	0.9028	10.44	3.793	8.63	0.151
7	1.273	0.9287	10.12	5.743	8.87	0.366
8	1.270	0.9550	9.874	8.670	8.62	0.738
9	1.267	0.9819	9.622	15.31	8.76	1.284
10	1.265	1.0073	9.290	28.73	9.13	2.09
11	1.264	1.034	8.963	62.85	9.45	3.14

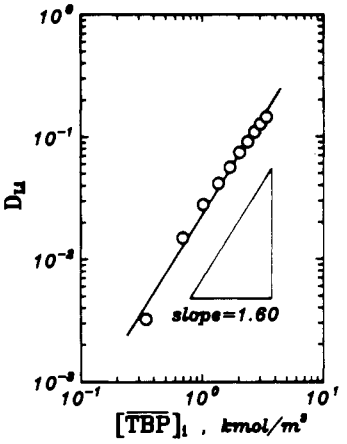

Figure 5. Variation of the distribution ratio with the concentration of TBP in the organic phase at $[LiCl]_i$ = 13.9 kmol/m³ and 25 °C.

kerosene solutions at 25 °C. Table V represents the densities, viscosities, and conductivities of the equilibrium aqueous phase and organic phase at constant initial LiCl concentration ($[LiCl]_i$ = 13.9 kmol/m³) and dilute concentrations of TBP dissolved in kerosene at 25 °C. A plot of the distribution ratios versus the concentration of TBP in organic solution is shown in Figure 5. The linear relationships between physical properties and concentrations of TBP can be expressed as

$$D_{LiCl} = 2.297 \times 10^{-2}[\overline{TBP}]_i^{1.603} \quad (7)$$

$$\rho_{aq} = (-9.907\ \text{kg/kmol})[\overline{TBP}]_i + 1295\ (\text{kg/m}^3) \quad (8)$$

$$\rho_{org} = (73.82\ \text{kg/kmol})[\overline{TBP}]_i + 779.3\ (\text{kg/m}^3) \quad (9)$$

$$[\overline{H_2O}] = 0.5490[\overline{TBP}]_i^{1.759} \quad (10)$$

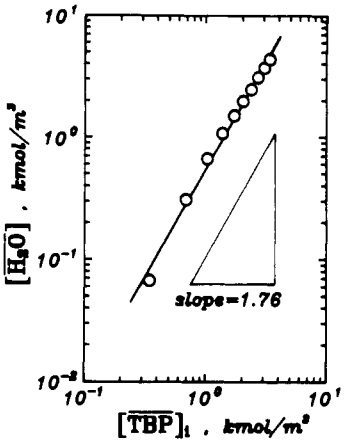

Figure 6. Variation of the water content with the concentration of TBP in the organic phase at $[LiCl]_i$ = 13.9 kmol/m³ and 25 °C.

A plot of water content against concentration of TBP in organic solutions is shown in Figure 6. The relationship of eq 10 is in accordance with the result of Alcock et al. (*13*).

Extraction Behavior. For the results described above, we can propose a series of reactions of lithium chloride and TBP from dilute to dense concentration of lithium chloride of aqueous solutions.

1. $[LiCl]_{aq} = 0$

$$\overline{TBP} + H_2O \rightleftharpoons \overline{TBP{\cdot}H_2O} \quad (11)$$

$$2\overline{TBP} + 2H_2O \rightleftharpoons \overline{(TBP)_2{\cdot}(H_2O)_2} \quad (12)$$

2. $0 < [LiCl]_{aq} < 6$ kmol/m³

$$LiCl + m\overline{(TBP)_2{\cdot}(H_2O)_2} \rightleftharpoons \overline{LiCl{\cdot}(TBP)_3{\cdot}(H_2O)_4} + (m - {}^3/_2)\overline{(TBP)_2{\cdot}H_2O} + (m - {}^5/_2)H_2O \quad (13)$$

3. 6 kmol/m³ < $[LiCl]_{aq}$ < 10 kmol/m³

$$LiCl + {}^3/_2\overline{(TBP)_2{\cdot}H_2O} + {}^5/_2H_2O \rightleftharpoons \overline{LiCl{\cdot}(TBP)_3{\cdot}(H_2O)_4} \quad (14)$$

4. 10 kmol/m³ < $[LiCl]_{aq}$ < saturated

$$LiCl + \overline{LiCl{\cdot}(TBP)_3{\cdot}(H_2O)_4} \rightleftharpoons \overline{LiCl_2{\cdot}(TBP)_3{\cdot}(H_2O)_4} \quad (15)$$

$$n\overline{(LiCl)_2{\cdot}(TBP)_3{\cdot}(H_2O)_4} \rightleftharpoons \overline{((LiCl_2{\cdot}(TBP)_3{\cdot}(H_2O)_4)_n} \quad (16)$$

From row 1 of Table III, it can be seen that the ratio of TBP:H_2O is unity. McKay et al. (*6*) proposed that the compositions of organic phase are $\overline{TBP{\cdot}H_2O}$ and $\overline{(TBP)_2{\cdot}(H_2O)_2}$. Therefore, eqs 11 and 12 are expected.

From the first break point of Figure 4 and row 10 of Table III, the composition of the organic phase is expected to be $\overline{(TBP)_2{\cdot}H_2O}$. And then, each lithium chloride molecule is accompanied by ${}^5/_2$ water molecules on passing from the aqueous phase into the TBP phase. Also, the plot of log D_{LiCl} against the logarithm of the initial concentration of TBP in the organic phase, as shown in Figure 5, has a slope of 1.60. Therefore, the stoichiometries of ${}^3/_2$ and ${}^5/_2$ are obtained in eq 14, and the composition of the complex of the organic phase is $\overline{LiCl{\cdot}(TBP)_3{\cdot}(H_2O)_4}$, which can be obtained either by mass balance of eq 14 or by the ratio of $[\overline{LiCl}]$:$[\overline{TBP}]$:$[\overline{H_2O}]$, which is approxi-

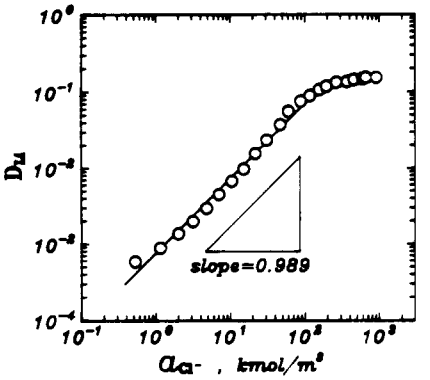

Figure 7. Distribution ratio versus the activity of lithium chloride in the equilibrium aqueous phase at $[\overline{TBP}]_i$ = 3.41 kmol/m³ and 25 °C.

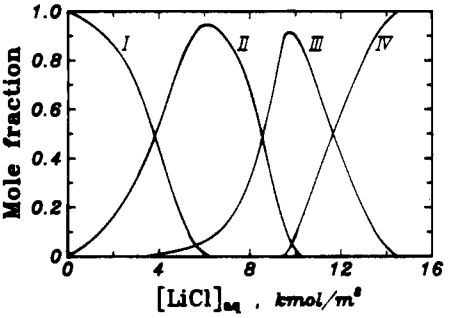

Figure 8. Lithium chloride and TBP distribution diagrams as a function of the equilibrium concentration of lithium chloride in the aqueous phase: (I) $\overline{TBP}$, (II) $\overline{TBP{\cdot}H_2O}$ + $\overline{(TBP)_2{\cdot}(H_2O)_2}$, (III) $\overline{LiCl{\cdot}(TBP)_3{\cdot}(H_2O)_4}$, and (IV) $\overline{(LiCl)_2{\cdot}(TBP)_3{\cdot}(H_2O)_4}$.

mately 1:3:4 from experiment no. 16 of Table III (i.e., the end point of the linear relationship in the second part of Figure 4).

Figure 7 shows the plot of distribution ratios of lithium chloride versus the activity of lithium chloride of aqueous solutions. The activity coefficients are obtained from Robinson and Stokes (*17*, *18*). The curve has a unit slope at $[LiCl]_{aq}$ < 10 kmol/m³, which means that the composition of the complex of the organic phase is identical at this range of concentration. Therefore, eq 13 is expected, and the stoichiometry coefficient, m, is decreasing with the concentration of lithium chloride increasing.

The last row of Table I indicates that the aqueous phase is maintained at saturation. The ratio of $[\overline{LiCl}]$:$[\overline{TBP}]$:$[\overline{H_2O}]$ is 2:3:4 from Table III; i.e., the composition of lithium chloride extracted in the organic phase is $\overline{(LiCl)_2{\cdot}(TBP)_3{\cdot}(H_2O)_4}$. The solvation number is 3.5 for the lithium chloride; that is consistent with the value of 3–4 in the literatures (*19*, *20*). From Figure 2, the viscosity of the organic phase increases rapidly when the concentration of lithium chloride reaches saturation, which indicates that polymerization of the extracted species takes place. Therefore, eqs 15 and 16 are obtained.

Conclusion

In the present study, extraction behavior of lithium chloride by TBP dissolved in kerosene has been investigated at 25 °C. The compositions of the organic phase are found to contain $TBP{\cdot}H_2O$, $(TBP)_2{\cdot}H_2O$, $(TBP)_2{\cdot}(H_2O)_2$, $LiCl{\cdot}(TBP)_3{\cdot}(H_2O)_4$, $(LiCl)_2{\cdot}(TBP)_3{\cdot}(H_2O)_4$, and $((LiCl)_2{\cdot}(TBP)_3{\cdot}(H_2O)_4)_n$. Figure 8 represents the distribution diagram of the complexes of LiCl and TBP in the organic phase as a function of the equilibrium concentration of lithium chloride in the aqueous phase.

Nomenclature

a = Activity, kmol/m³
D = distribution ratio
m,n = stoichiometry coefficient
— = organic phase species or organic phase concentration

Greek Letters

α = degree of dissociation
κ = conductivity, 1/(Ω·m)
Λ = equivalent conductance, m²/(Ω·kmol)
η = viscosity of solution, kg/(m·s)
ρ = density of solution, kg/m³

Subscripts

aq = aqueous phase
eq = equilibrium state
i = initial condition
org = organic phase

Literature Cited

(1) Sekine, T.; Hasegawa, Y. *Solvent Extraction Chemistry: Fundamentals and Applications*; Marcel Dekker: New York and Basel, 1977.
(2) Ritcey, G. M.; Ashbrook, A. W. *Solvent Extraction: Principles and Applications to Process Metallurgy*; Elsevier: Amsterdam, 1984; Part II.
(3) Huang, T. C.; Huang, C. T. *J. Membr. Sci.* **1986**, *29* (3), 295.
(4) Baldwin, W. H.; Higgins, C. E.; Soldano, B. A. *J. Phys. Chem.* **1959**, *63*, 118.
(5) Morris, D. F. C.; Short, E. L. *J. Inorg. Nucl. Chem.* **1963**, *25* (3), 291.
(6) McKay, H. A. C.; Hardy, C. J.; Fairhurst, D.; Wilson, A. M. *Trans. Faraday Soc.* **1962**, *58*, 1626.
(7) Roddy, J. W. *J. Inorg. Nucl. Chem.* **1978**, *40* (10), 1787.
(8) Fischer, K. *Angew. Chem.* **1935**, *48* (26), 394.
(9) Huang, T. C.; Tsai, T. H. *Ind. Eng. Chem. Res.* **1989**, *28* (10), 1557.
(10) Fajans, V. K.; Hassel, O. *Z. Elektrochem.* **1923**, *29*, 495.
(11) Wilson, C. L.; Wilson, D. W. *Comprehensive Analytical Chemistry*; Elsevier: Amsterdam, 1962; Vol. IB.
(12) McKay, H. A. C.; Mathieson, A. R. *Trans. Faraday Soc.* **1951**, *47*, 428.
(13) Alcock, K.; Grimley, S. S.; Healy, T. V.; Kennedy, J.; McKay, H. A. C. *Trans. Faraday Soc.* **1956**, *52*, 39.
(14) Tuck, D. G. *J. Chem. Soc.* **1958**, 2783.
(15) Kertes, A. S. *J. Inorg. Nucl. Chem.* **1960**, *14*, 104.
(16) Katzin, L. I.; Sullivan, J. C. *J. Phys. Colloid Chem.* **1951**, *55*, 346.
(17) Robinson, R. A.; Stokes, R. H. *Trans. Faraday Soc.* **1949**, *45*, 612.
(18) Robinson, R. A.; Stokes, R. H. *Electrolyte Solutions*, 2nd. rev. ed.; Butterworths: London, 1970.
(19) Kielland, J. *J. Am. Chem. Soc.* **1937**, *59*, 1675.
(20) Stokes, R. H. In *The Structure of Electrolytic Solutions*; Hamer, W. J., Ed.; Wiley (Chapman Hall): New York (London), 1959; p 298.

Received for review July 17, 1990. Accepted January 31, 1991. This work was performed under the auspices of the National Science Council of the Republic of China, under Contract No. NSC77-0402-E006-05, to which we express our thanks.